Vol. 144: 223-236, 1996 | MARINE ECOLOGY PROGRESS SERIES Mar Ecol Prog Ser | Published December 5

An *in situ* biological weighting function for UV inhibition of phytoplankton carbon fixation in the Southern Ocean

Nicolas P. Boucher[1,*], Barbara B. Prézelin[2]

[1]Laboratoire d'Ecologie Marine, Université de la Réunion, F-97715 Saint Denis Messag, France
[2]Marine Primary Production Group, Department of Biological Sciences, University of California, Santa Barbara, California 93106, USA

ABSTRACT: A daily integrated *in situ* biological weighting function (BWF) for inhibition of primary production by ultraviolet radiation (UVR, 280 to 400 nm) was determined for a natural community of Antarctic diatoms maintained under daylight conditions. The derived daily averaged BWF had a radiation amplification factor of 0.91 for the environmental radiation conditions under which it was determined, and displayed greater sensitivity to UV-B than BWFs determined for laboratory cultures of temperate latitude phytoplankton (Cullen et al. 1992; Science 258:646–650). In addition, the function was shown to accurately predict the UVR-dependent *in situ* rates of primary production when the same community was under different stratospheric ozone (O_3) conditions. An error estimate for the BWF is also provided and the predictive limitations of the function are discussed briefly. In the early austral spring of 1993 near Palmer Station, Antarctica, surface samples were maintained in 6 spectrally distinct outdoor incubators over the course of a single day and the spectral sensitivity of photosynthetic carbon fixation rates and phytoplankton pigmentation was quantified. The changes in spectral sensitivity to O_3-dependent UV-B (280 to 320 nm radiation) and O_3-independent UV-A (320 to 400 nm radiation) was resolved on time scale of 2 h intervals over the course of the 10 h incubation. Besides determining the daily peak of cell sensitivity to UVR damage, the derived short-term kinetics for the 6 different spectral light treatments provided the database for resolving a robust action spectrum for the UVR inhibition of *in situ* rates of primary production. For the diatom community being studied, daily exposure to ambient levels of UVR resulted in a 34% reduction in averaged carbon fixation without any significant effect on the cellular pigment content. The UV-B portion of the solar spectrum photoinhibited daily rates of primary production by 15%, while UV-A was responsible for a 19% reduction in daily averaged rates of carbon fixation. It appears that springtime diatom-dominated communities are equally or more sensitive to UV-B photoinhibition of daily primary production than prymnesiophyte-dominated communities, analyzed during the 1990 'Icecolors' expedition (Smith et al. 1992; Science 258:952–959).

KEY WORDS: UV · Primary production · Phytoplankton · Antarctica · Action spectra · Photoinhibition · Ozone

INTRODUCTION

It is widely acknowledged that the severity (i.e. magnitude, area and duration) of the Antarctic ozone (O_3) 'hole' has increased significantly in the last decade. It is now common to observe springtime O_3 levels 30 to >50% less than levels measured pre-O_3 hole or at lower latitudes 'outside' the O_3 hole [ca >250 to 400 Dobson Units (DU)] (Smith et al. 1992, Stolarski et al. 1992, Madronich 1993, Booth et al. 1994). The maximum area covered by the O_3 hole has expanded nearly to the limit of the south polar vortex and routinely passes over the majority of the Southern Ocean. In addition, O_3-poor air masses commonly reach South America and Australia (Roy et al. 1994). The duration of the O_3 hole appears to be lengthening: while the depletion was first observed only in October, it has lately been evident from late September until early

*E-mail: boucher@univ-reunion.fr

December. In 1993, the magnitude of the O_3 hole was remarkable in that stratospheric O_3 levels over the South Pole were the lowest on record (<100 DU) and significant O_3 depletion was observed over large regions of the Antarctic continent prior to the beginning of spring (WMO 1995). All of the above changes, as well as the observations that O_3 levels are declining (although less severely) over much of the rest of the world are consistent with reports that the global inventory of O_3 has decreased in recent years (Stolarski et al. 1992).

The direct link between O_3 depletion, increased UV-B irradiance (E_{UVB}, 280 to 320 nm), and associated changes in the spectral balance of UV-B, UV-A and photosynthetically available radiation (PAR) (Table 1), has raised concern and prompted research into the potential impacts of environmental increases in E_{UVB} on the ecological balance of Antarctica (Weiler & Penhale 1994). Given that the vast majority of Antarctic communities are marine and dependent upon the productivity of phytoplankton, and that the timing of the greatest relative increase in E_{UVB} coincides with the spring growing season, the impact of ultraviolet radiation (UVR) on autotrophic carbon fixation in the Southern Ocean has received special attention in recent years (El-Sayed et al. 1990, Karentz et al. 1991a, b, Helbling et al. 1992, Smith et al. 1992, Holm-Hansen et al. 1993, Prézelin et al. 1994b, Weiler & Penhale 1994). While laboratory studies have a place in defining mechanisms of E_{UVB} damage, it is increasingly recognized that environmental concerns, and their possible remediation, cannot be addressed adequately until O_3-related effects are quantified and evaluated under natural conditions (see UNEP 1994). Relevant field experiments, Prézelin et al. (1994a) argued, had to consider that phytoplankton are polychromatic organisms. Modifying the spectral balance of their light fields on time scales of a few hours to days as the O_3 hole oscillates overhead could easily upset the balance of the many interdependent photoprocesses (photosynthesis, photorepair, photoadaptation, nitrogen assimilation, taxis etc.) that all plants have evolved over millennia (Mohr et al. 1984, Senger et al. 1986, Middleton & Teramura 1994).

Whereas the spectral increase in UV-B associated with the reduction in stratospheric O_3 is well documented (Lubin & Frederick 1991, Madronich 1993), the effects of the spectral shifts in UV radiation on primary production remain less well understood. Action spectra linking the amount of damage to the wavelength of UVR have long been measured for several photoprocesses in terrestrial animal and plant physiology (Caldwell et al. 1986), but it is only recently that such functions have been described for temperate phytoplanktonic organisms (Cullen et al. 1992). With the advent of the ozone hole, the shape of such spectra has been used as a biological weighting function (BWF) to compensate for the unbalanced effects of UVR on biological systems and quantify a radiation amplification factor (RAF), i.e. the increment of biological damage associated with a diminution in O_3 concentration (National Academy of Sciences 1979, Madronich & de Gruijl 1993, Booth & Madronich 1994). An important step to improve predictive models of Antarctic phytoplankton productivity in UV-enhanced environments is to determine the sensitivity of natural communities

Table 1. Significant symbols and abbreviations

C	Carbon (mg m^{-3})
Chl	Chlorophyll *a* (mg m^{-3})
$Q(\lambda)$	Quantum irradiance at wavelength λ (µmol quanta m^{-2} s^{-1})
$E(\lambda)$	Irradiance at wavelength λ (W m^{-2})
PAR	Photosynthetically available radiation (400–700 nm)
UVR	Ultraviolet radiation (280–400 nm)
UV-A	Ultraviolet A radiation (320–400 nm)
UV-B	Ultraviolet B radiation (280–320 nm)
$\varepsilon(\lambda)$	Biological weighting function (BWF) at wavelength λ
RAF	Radiation amplification factor
AI_{Tnm}	Absolute inhibition of primary production in spectral incubator Tnm
FI_{Tnm}	Fractional UV inhibition of primary production in spectral incubator Tnm
α	Photosynthetic efficiency [mg C m^{-3} h^{-1} (µmol quanta m^{-2} s^{-1})$^{-1}$]
β	Slope of the white light photoinhibited portion of the *P-I* curve [mg C m^{-3} h^{-1} (µmol quanta m^{-2} s^{-1})$^{-1}$]
I_k	Minimum irradiance for onset of light-saturated rates of photosynthesis (µmol quanta m^{-2} s^{-1}) (= P_{max}/α)
I_t	Minimum irradiance for onset of white light inhibition of photosynthesis (µmol quanta m^{-2} s^{-1}) (= P_{max}/β)
P_{max}	Volume-specific rate of light-saturated photosynthesis (mg C m^{-3} h^{-1})
P_{max}/chl	Chl-specific rate of light-saturated photosynthesis (mg C mg chl^{-1} h^{-1})
P	Volume-specific rates of *in situ* photosynthesis (mg C m^{-3} h^{-1})
P/chl	Chl-specific rates of *in situ* photosynthesis (mg C mg chl^{-1} h^{-1})
P_i	Photosynthetic rate modelled from *P-I* parameters (mg C m^{-3} h^{-1})
P_{PAR}	Photosynthetic rate under PAR only (mg C m^{-3} h^{-1})
P_{Tnm}	Photosynthetic rate in the incubator Tnm (mg C m^{-3} h^{-1})
Tnm	Incubator designation based on a filter combination that transmits ≥ 50% of incoming light at wavelengths > 'nm'

to spectral shifts in ambient UVR, i.e. the BWF, and therefore link changes in E_{UVB} (i.e. due to season, time of the day, cloud and ice cover, stratospheric O_3 concentration and location in the water column) to the inhibition of carbon uptake in Antarctic phytoplankton.

The present experiment was conducted to estimate the *in situ* daily integrated BWF for primary production inhibition in Antarctic phytoplankton under natural irradiance conditions. We quantified the inhibitory effects of different bandwidths of UVR on springtime primary production of typical Antarctic coastal waters diatom communities. Here, we present and test the function, demonstrate that the sensitivity of Antarctic phytoplankton to UV-B during the early spring transition to higher irradiances is greater than that of temperate terrestrial plants and marine phytoplankton, and show how the newly derived *in situ* BWF can be used to model UV-dependent rates of primary production for similar diatom-dominated communities. We make no assumption regarding the universality of our BWF, as such conclusions can not be reached until more field data are available.

MATERIAL AND METHODS

Location and time of work. Measurements were made on September 16, 1993 [Day 259 of the Year] in ice-free coastal waters of the Antarctic Peninsula. Working from a Mark V Zodiac near dawn (ca 08:00 h local time, LT), a large volume (20 l) of surface water was collected in blackened polyethylene bottles at the Palmer Long Term Ecological Research (LTER) Station B (64° 46.77' S, 64° 4.35' W). Bottles were returned to the laboratory within 30 min of collection, and samples prepared for outdoor incubations in less than 1 h.

Outdoor simulated *in situ* (SIS) incubators. Optical notations and other significant symbols and abbreviations are defined in Table 1. Outdoor SIS incubators described elsewhere (Prézelin et al. 1994b) were employed for determination of the BWF, thereby assuring that samples were exposed to the natural fluctuations in the solar light field over the course of a day. For the different spectral light treatments, the containers and the sample compartment dividers were composed of black Plexiglas to eliminate back and side direct radiation and to minimize reflection. Trays were covered with combinations of long-pass filters selected to remove increasingly larger portions of the UV spectrum.

For each of the treatments, 18 ^{14}C radiolabelled 200 ml samples and 3 non-radiolabelled 500 ml samples were sealed in nontoxic UV-transparent polyethylene (PE) bags (Prézelin et al. 1994a, b). Once filled, the sample bags had the broad sides exposed to the incoming light field and were in direct contact with incubator lids. A constant flow of sea water was pumped from the nearby harbor and circulated through the incubators keeping the SIS samples within 0.5°C of *in situ* surface water temperature.

Spectral attenuation within each light treatment. Knowledge of the transmission characteristics of the incubators and the fluctuating environmental spectral irradiance was required to accurately estimate the phytoplankton exposure within each bag and for any time interval within the day. The optical properties of the different filter materials and the PE bags were determined on a DW-2 Aminco spectrophotometer (0.67 nm resolution) and are presented in Fig. 1. For clarity, the term 'Tnm' is used here to designate each light treatment by its 50% transmittance wavelength, i.e. T299 denotes the light treatment transmitting 50% of 299 nm light and more than 50% all wavelengths greater than 299 nm.

Spectrally integrated PAR (Q_{PAR}, µmol quanta m^{-2} s^{-1}) was monitored continuously using a Biospherical 185B photometer placed next to the outdoor incubator

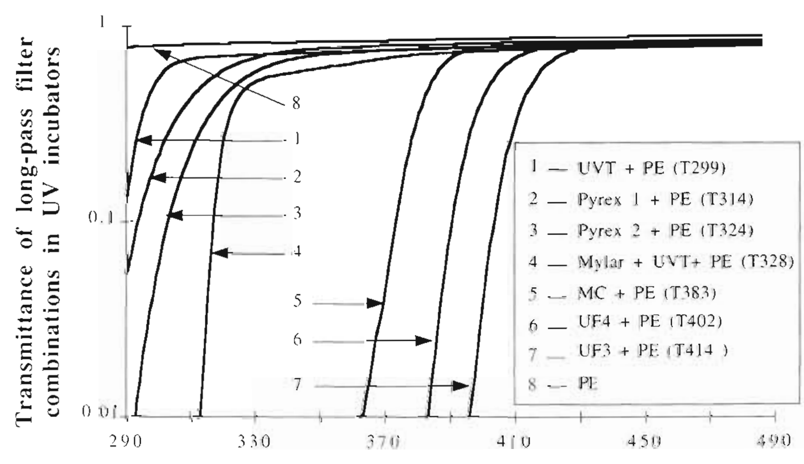

Fig. 1 Comparison of the UVR transmission properties for samples sealed in polyethylene (PE) incubation bags and placed within different spectral incubators during the 'Icecolors 93' field expedition. The rigid long-pass filters consisted of 6.4 mm Plexiglas (UVT, MC, UF4, UF3), or 3.2 mm UVT Plexiglas when used in combination with an inserted 0.13 mm sheet of Mylar (Mylar), 6.4 mm (Pyrex 2) and 3.2 mm(<Pyrex 1) Pyrex. The resulting 50% transmission cutoffs wavelengths and average transmission in the PAR region were: (1) <290 nm and 91.2%; (2) 299 nm and 83.0%; (3) 314 nm and 86.8%; (4) 324 nm and 82.9%; (5) 328 nm and 81.4%; (6) 382 nm and 84.2%; (7) 402 nm and 84.6%; (8) 414 nm and 79.5%. For added details regarding outdoor incubators, see Prézelin et al. (1994a, b)

and 5 min averages recorded on a Li-Cor 1000 datalogger. In addition, the NSF (National Science Foundation) polar network for monitoring UV radiation (Booth et al. 1994) provided spectral irradiance at the surface measured every hour, on the hour [$E_d(\lambda, 0^+)$, λ = 280 to 400 nm, 0.1 nm step size]. Radiation inside the experimental containers was determined by multiplying the irradiance spectra by the transmission spectra of the incubator. For all calculations, transmittance spectra were numerically degraded to 1 nm resolution.

Chemical analyses. Chlorophyll *a* (chl) and accessory pigments as well as particulate carbon (C) and nitrogen (N) concentrations were measured at the sampling site for 3 d prior to the experiment. CN samples (1.5 l) were filtered onto pre-combusted (1 h at 500°C) Whatman GF/F glass fiber filters, dried at 65°C and transported to the Marine Science Analytical Laboratories at UC Santa Barbara, CA, USA, where chemical analyses where made using standard techniques (see Moline et al. 1997, and references within).

Phytoplankton pigmentation was determined by high performance liquid chromatography (HPLC) on a Hitachi HPLC system and using procedures described elsewhere (Prézelin et al. 1992, Moline et al. 1997). Pigment determinations were done on the freshly collected *in situ* material, the sample retrieved from each incubator at the end of the incubation and a series of samples retrieved every 2 h from T299, which most closely mimics *in situ* conditions. Triplicate sea water samples (500 ml each) were collected at each sampling interval, pooled, filtered onto 0.4 µm 47 mm Nalgene nylon filters and frozen at –70°C for at least 2 h. At the time of analysis, pigments were extracted in 90% acetone at 0°C for 18 h and the extracts were centrifuged to remove non-pigmented material.

$H^{14}CO_3^-$ procedures for indoor photosynthetron measurements. Photosynthesis-irradiance (*P-I*) relationships were measured in indoor blue-light photosynthetrons every 2 h for the samples incubated under the full solar spectrum (T299) For each *P-I* determination, a 30 ml subsample was removed from the non-radiolabelled T299 sample and inoculated with $H^{14}CO_3^-$ to a final concentration of 9 µCi ml^{-1} Then, 25 discrete samples, 1 ml each, were aliquoted into glass scintillation vials, placed in temperature-controlled photosynthetrons and incubated for 2 h. Light was provided by a set of tungsten lamps illuminating samples through an overlying plastic chamber filled with a 1% $CuSO_4$ aqueous solution. This filter/solution combination decreased the heat load on the sample (infrared radiation), removed any incoming UV radiation and provided a better spectral match with the *in situ* PAR. As such, the filter/solution combination attempted to correct the artificially unbalanced light fields common to unfiltered tungsten white light fields (Prézelin et al. 1989, Schofield et al. 1991). Q_{PAR} values in the photosynthetrons ranged from 4 to 1100 µmol quanta m^{-2} s^{-1} and were adjusted when necessary by using combinations of neutral density plastic filters.

At the end of the incubation, the samples were acidified (glacial acetic acid/methanol, 1/30 v/v) and heat dried for 24 h at 65°C (Prézelin et al. 1987). One ml of distilled water was added to the samples to dissolve salts. Five ml of Ecoscint scintillation cocktail were added and samples vortexed to complete mixing prior to determination of the disintegration rate (DPM). Volumetric primary production (mg C m^{-3} h^{-1}) was calculated from the sample DPM and the total activity prior to the incubation as described by Parsons et al. (1984).

The *P-I* parameters describing the relationship between photosynthesis and irradiance were derived using the relationships (Neale et al. 1987):

$$P_i = P_{max} \tanh\left(\frac{Q_{PAR}}{I_k}\right) \quad \text{for } Q_{PAR} \le I_t$$

and (1)

$$P_i = P_{max} \exp[-\beta(Q_{PAR} - I_t)] \quad \text{for } Q_{PAR} > I_t$$

where P_i is the instantaneous rate of primary production (mg C m^{-3} h^{-1}), P_{max} is the light-saturated photosynthetic potential, I_k is the minimum light requirement for the onset of light-saturation of photosynthesis (and is equal to P_{max}/α, where α is the photosynthetic efficiency), β is the photoinhibition rate, and I_t is the minimum light requirement for the onset of Q_{PAR} photoinhibition (= P_{max}/β). Error estimates for each parameters were determined as described by Zimmermann et al. (1987).

$H^{14}CO^{3-}$ procedures for *in situ* BWF measurements. Measurements of SIS rates of carbon fixation were made in the outdoor incubators for 6 light treatments (T299, T314, T324, T328, T382, T402). The T414 incubator was not used in the BWF determination on September 16, due to technical difficulties on that day. A 13 l sample was inoculated with $H^{14}CO_3^-$ to a final concentration of 0.5 µCi ml^{-1}. Aliquots, each 200 ml, were quickly dispensed into PE bags and placed in outdoor incubators at 09:35 h LT.

To determine the time course of carbon uptake over a single day, duplicate samples were removed from each incubator every hour from 10:00 to 18:00 h LT, fixed with 0.5% formalin and gently filtered onto a 0.4 µm Nuclepore filter rinsed with filtered sea water. Sample DPMs were measured after placing each filter in Ecoscint scintillation cocktail. All carbon fixation rates were corrected for dark fixation. Volumetric primary production was calculated as described in the previous section.

Absolute inhibition (AI) and fractional inhibition (FI) calculations. The light treatments represent overlapping radiation regimes of progressively larger

bandwidths. The inhibition in each incubator was calculated by subtraction: the volumetric carbon uptake rates in the sample exposed to PAR only (P_{T402}, mg C m^{-3} h^{-1}) was used as reference to compute the absolute inhibition (AI_{Tnm}, mg C m^{-3} h^{-1}) as follows

$$AI_{Tnm} = P_{T402} - P_{Tnm} \quad (2)$$

where P_{Tnm} is the primary production measured in incubator Tnm. The fractional inhibition (FI_{Tnm}, unitless) is then equal to:

$$FI_{Tnm} = 1 - \frac{P_{Tnm}}{P_{T402}} \quad (3)$$

Analytical approach to BWF determination. We assumed that the fractional inhibition FI_{Tnm} over a time interval can be expressed as a function of the average irradiance [$E(\lambda)_{Tnm}$, W m^{-2}] which impinges on the phytoplankton community inside the incubator and the BWF [$\varepsilon(\lambda)$, (W m^{-2})$^{-1}$], representing the spectral sensitivity of the organism to such radiation, such that:

$$FI_{Tnm} = \Sigma_{UVR} E(\lambda)_{Tnm}\, \varepsilon(\lambda)\, d\lambda \quad (4)$$

A similar equation can be written for the absolute inhibition AI_{Tnm} (mg C m^{-3} h^{-1}) as:

$$AI_{Tnm} = 3600\, \Sigma_{UVR} E(\lambda)_{Tnm}\, \varepsilon^{\bullet}(\lambda)\, d\lambda \quad (5)$$

where $\varepsilon(\lambda)^{\bullet}$ has units of mg C m^{-3} (J m^{-2})$^{-1}$ and is related to $\varepsilon(\lambda)$ by the constant factor P_{T402}.

Since FI_{Tnm} determinations are broad band measurements, the sensitivity function $\varepsilon(\lambda)$ can not be mathematically derived from Eq. (4) alone. However, the method outlined by Rundel (1983) can be used to extract the spectral dependency of the function from knowledge of the several broad band FI_{Tnm}. Assuming a mathematical form of the BWF $\varepsilon(\lambda)$, one can calculate the expected fractional inhibitions $FI_{exp,Tnm}$ for each time interval and in each incubator Tnm from the average irradiance $E(\lambda)_{Tnm}$ (Eq. 4). The best-fit $\varepsilon(\lambda)$ is obtained when the mean squared error [$\chi^2 = \Sigma_i (FI_{exp,i} - FI_i)^2/(FI_{exp,i})$, i = T299, T314, T324, T328 and T383] is minimized. We used iterative non-linear fitting techniques to minimize χ^2 by varying the parameters describing $\varepsilon(\lambda)$. With 5 data points available in our experiment (6 filters giving 5 FI_{Tnm} values), the number of adjustable parameters describing $\varepsilon(\lambda)$ is limited to 4. As a result, only simple equations can be used and fine-scale resolution will be lost. Since the sensitivity of various organisms to UVR has been shown to decrease exponentially with wavelength (Rundel 1983), the best-fit BWF was chosen from results obtained using increasingly complex exponential decay functions.

The accuracy of this deconvolution technique increases with the number of filters used and depends on the distribution along the UV region of the spectrum of the transmittance cut-offs of the filters. To compensate for the limited number of suitable long-pass filters, we concentrated the highest resolution in the UV-B region of the spectra, where the slope of the BWF has been shown to vary the most for other plant photoprocesses (Caldwell 1986) and where findings would have greatest significance to assess the effects of changing O_3-dependent UV climatology on marine primary production.

RAF determination. The sensitivity of a given photoprocess to a decrease in O_3 concentration can be described by a single parameter, the radiation amplification factor (RAF). RAF is a measure of the relative increase in biologically effective UVR for a given level of O_3 reduction. It has recently been mathematically described for large variations in O_3 concentration by Madronich (1993) using the power formulation:

$$\frac{AI_j}{AI_{360}} = \left(\frac{N_{360}}{N_j}\right)^{RAF} \quad (6)$$

where AI_j and AI_{360} are the inhibition corresponding to ozone concentration of j DU (N_j) and 360 DU (N_{360}). The best-fit value for RAF was calculated for N varying between 100 and 360 DU in 10 DU increments. The corresponding inhibition values were determined using Eq. (5), with input data for daily average solar irradiances obtained from the clear-sky model of Madronich (1993) applied to September 16 at a latitude of 64° S.

RESULTS

Physical environment

In 1993, the ozone hole over Antarctica developed very early. At the beginning of August, the stratospheric O_3 above Palmer Station had already reached column concentrations below 200 DU (Fig. 2), an arbitrary value previously used to define the outer boundary of the O_3 hole (Smith et al. 1992). On September 16, the fourth passage of the hole over Palmer Station since the start of our field program was observed. The spring growing season was therefore initiated with an enhanced level of UV-B. The potential UV-B exposure was increased further at our study site as the area was virtually ice-free throughout the months of August and September 1993.

On September 16 (Day 259 of the Year), the O_3 concentration was 260 DU, in the middle of a 3 d transition period from 180 to 320 DU as the O_3 hole moved away from the site (Fig. 2). While the amount of UV-B radiation reaching the earth surface was slightly enhanced due to the O_3 diminution, it was still low due to the large solar zenith angle. However, daylength was increasing rapidly (ca 20 min d^{-1}) and on September

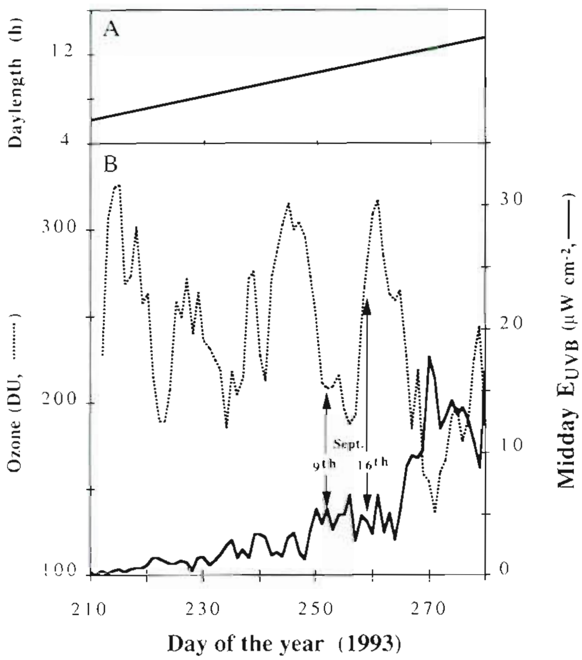

Fig. 2. Changes in (A) daylength and (B) stratospheric ozone column concentration (DU) above Palmer Station, Antarctica (Meteor 3 TOMS data) and midday (16:00 h GMT) UV-B (280 to 320 nm) irradiance (μW cm^{-2}) at Palmer Station during the first half of the 'Icecolors 93' expedition. Arrows indicate: date when a daily averaged biological weighting function (BWF) for UV inhibition of *in situ* primary production was determined (September 16, 1993, Day of the Year 259) for surface water phytoplankton; and date (September 9, 1993, Day of the Year 252) when data was collected to test the BWF ability to predict UV inhibition of *in situ* primary production under different levels of stratospheric O_3 concentrations

16, the photoperiod was 11 h 25 min long, with sunrise occurring at 06:20 h LT and sunset at 17:45 h LT

Weather perturbations, typical of episodic patterns routinely experienced in Antarctica on the time scale of a single day, caused significant fluctuations in the natural light field (Fig. 3). While solar radiation generally increased with decreasing solar zenith angle, maximum quantum flux occurred before solar noon (12:00 h LT) on September 16. Early morning hours were characterized by completely overcast skies, clearing intermittently in late morning when the maximum $Q_{PAR}(0^+)$ was recorded and approached 700 μmol quanta m^{-2} s^{-1} (Fig. 3A). Sudden white-out conditions occurred from a passing blizzard between noon and ca 14:00 h LT. Skies were clear for the last 2 h of daylight.

Monitoring of the UV spectral irradiances was limited to once an hour, on the hour. Sampling frequency was adequate to measure the major diurnal variations in total UV-A and total UV-B radiation. Fig. 3B shows the sharp decrease at 12:00 h LT, the shoulders at 14:00 h LT, when the blizzard stopped and at 16:00 h LT after the complete clearing. Under clear-sky conditions, the E_{UVB}:E_{UVA} ratio increase with solar zenith angle to a midday maximum. The E_{UVB}:E_{UVA} ratio over the day shows that the relative proportion of UV-B radiation was greatest and relatively stable between 11:00 and 14:00 h LT (Fig. 3B).

While the incubated samples were kept at a constant temperature due to high volume circulation of surface sea water, the outside air temperature ranged from −11.5 to −6.5°C with an average of −8.8°C. Constant attention was given to the incubators and light sensor to assure proper functioning of the equipment at these low temperatures and during snowfall. The easterly winds (230°) peaked at 31 knots (15.5 m s^{-1}) in the afternoon blizzard and averaged 9 knots (4.5 m s^{-1}) over the day.

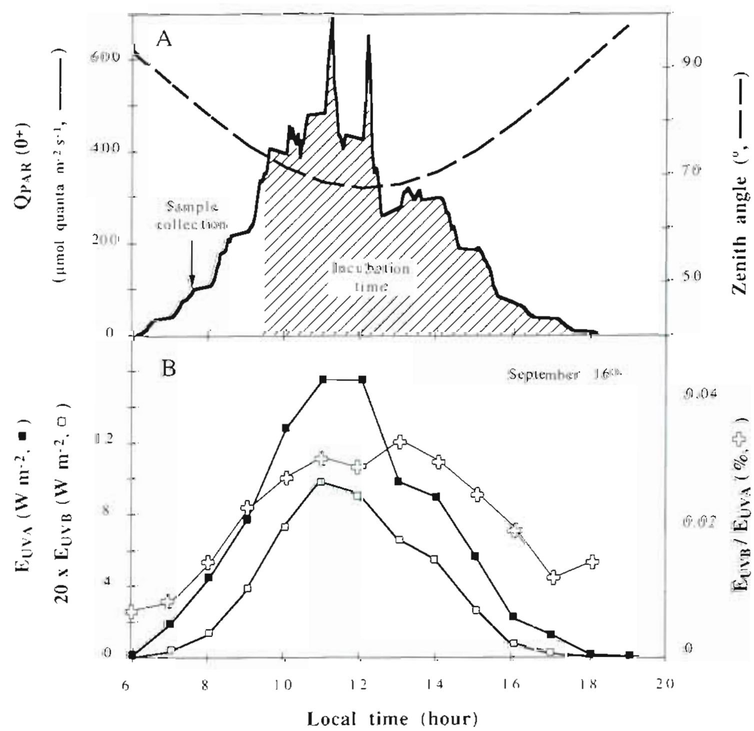

Fig. 3. Solar light conditions on September 16, 1993, when the BWF or UV inhibition of *in situ* primary production was determined. (A) Comparison of daytime variation in PAR quantum irradiance at the surface [$Q_{PAR}(0^+)$] and zenith angle with the arrow indicating the time of field collection and the shaded area under the Q_{PAR} curve indicating the outdoor incubation period. (B) Comparison of daytime variations in UV-A (E_{UVA}, 320 to 400 nm), UV-B radiation (E_{UVB}, 280 to 320 nm) and the E_{UVB} to E_{UVA} ratio (note the change of scale)

Photosynthetic parameters

Hydrographic, optical and pigment profiles of the *in situ* characteristics of the water column made at the time of sampling, as well as several days before and after sampling, confirmed that the experimental sample, while dilute (0.195 mg chl m^{-3}), was representative of the late winter/early spring phytoplankton communities (Prézelin unpubl.). The presence of fucoxanthin as the main photosynthetic pigment (fucoxanthin/chl = 0.49 w/w) confirmed the microscope observation that the surface phytoplankton community was dominated by diatoms, commonly found at this time of the year within the near shore region of Arthur Harbor (Krebbs 1983).

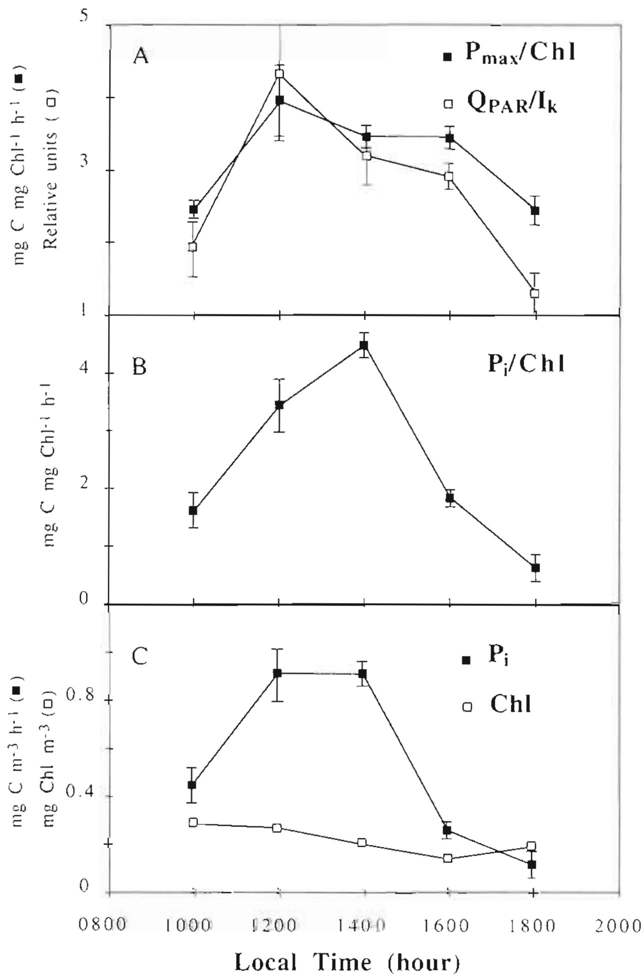

Fig. 4. Diurnal variation in the photophysiology of Antarctic surface phytoplankton maintained in the full spectral incubator (T299) under simulated *in situ* conditions on September 16, 1993. (A) Comparison of derived estimates of the light saturation index (ratio of incident photosynthetically available radiation Q_{PAR} to the minimum light requirement to saturate photosynthesis I_k) and the chl-specific light-saturated rate of photosynthesis (P_{max}/chl, mg C mg chl^{-1} h^{-1}). (B) Diurnal variation in derived rates of photosynthetic performance (P_i/chl, mg C mg chl^{-1} h^{-1}). (C) Comparison of daytime changes in volumetric production rate (P_i, mg C m^{-3} h^{-1}) and the chlorophyll concentration (chl, mg m^{-3}). Error bars represent the estimate of ± 1 SD around the derived parameters

Knowledge of the diurnal variation of photosynthetic characteristics of the population provides necessary information to assess the success of simulated *in situ* experiments, to document the physiological state of the natural community during the incubation and to provide intercomparable rates of primary production. The diurnal variations in light-saturated and light-limited rates of chl-specific photosynthesis were monitored every 2 h by measuring *P-I* curves in indoor PAR-only incubators (photosynthetrons), from samples exposed to full solar radiation (T299). Chl-specific rates of light-saturated photosynthesis showed P_{max}/chl to vary 4-fold over the day with a peak value of 3.94 ± 0.57 mg C mg chl^{-1} h^{-1} measured close to solar noon (Fig. 4A). The minimum PAR required to saturate photosynthesis (I_k) varied 2-fold over the day (data not shown). Midday values averaged 109 ± 11 µE m^{-2} s^{-1} and decreased to 57 ± 9 µE m^{-2} s^{-1} before sunset. The ratio of incident irradiance Q_{PAR} to I_k varied between 1 and 4, clearly indicating that surface phytoplankton photosynthesis was light-saturated during most of the day and rarely inhibited by bright white light ($Q_{PAR}/I_k > 4$; Lewis et al. 1984). Light limitation ($Q_{PAR}/I_k < 1$) occurred only in the first and last hour of sunlight (Fig. 4A). Chl-specific photosynthetic efficiency (α/chl) was nearly constant during the first half of the day [0.03 mg C mg chl^{-1} h^{-1} (µE m^{-2} s^{-1})$^{-1}$, n = 3] increasing at the end of the day when the cells became light-limited (data not shown).

As modeled using Eq. (1), the chl-specific rates of photosynthesis (P_i/chl, Fig. 4B) and volumetric production rates (P_i, Fig. 4C) followed the diurnal pattern in irradiance with midday maximum of 4.5 mg C mg chl^{-1} h^{-1} and 0.91 mg C m^{-3} h^{-1}, respectively. Volumetric and chl-specific rates of production covaried over the day due to the relative constancy of chl abundance over the time course of the experiment.

Simulated *in situ* carbon uptake under 6 spectral treatments

The time course of cumulative carbon fixation (mg C m^{-3}) by the phytoplankton assemblages exposed to the 6 spectral light treatments is shown in Fig. 5. Error bars represent the range of values for the duplicate measurements. For all treatments over most of the day, cumulative volumetric production increased with the rate of increase being greatest near midday when Q_{PAR} was greatest. For all UV treatments (1 to 5), the cumulative radiolabelled carbon declined during the last hour of daylight.

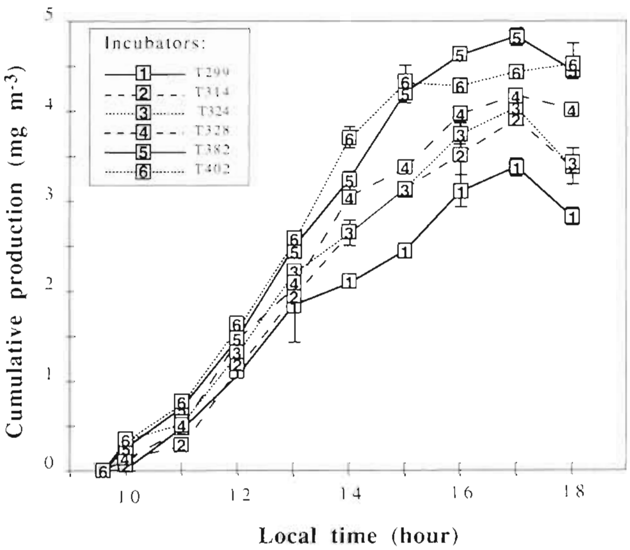

Fig. 5. Comparison of the time course of cumulative primary production (mg C m^{-3}) under the 6 UV spectral treatments used on September 16 and described in Fig. 1. Error bars represent the range of duplicate measurements

Under the experimental conditions, divergence in cumulative fixed carbon between different spectral treatments was significant after 2.5 h of incubation. Accumulation of radiolabelled carbon was enhanced by the removal of shorter bandwidths of UVR (Fig. 5). Samples exposed to unfiltered radiation (T299) showed the lowest uptake rates whereas primary production was highest in the Q_{PAR}-only treatment (T402) or Q_{PAR} with the addition of the longest wavelengths of UV-A (T383).

Average volumetric primary production, assimilation rates and doubling times in each UV treatment over the incubation time are summarized in Table 2. The doubling times estimates obtained from carbon fixation measurement on samples incubated under Q_{PAR} (T402, 3.9 d) and from *P-I* modeled estimates (3.8 d) were similar. The progressive addition of shorter UVR increased the community generation time to 6.3 d for the cells exposed to full incident UVR.

Estimates of the daily average UV inhibition of carbon fixation rates in each treatment were obtained by regressing primary production measured at each time interval in each incubator with the primary production measured under Q_{PAR} only (Fig. 6A). Such a normalization procedure eliminated considerations of the diurnal Q_{PAR}-dependent variation of primary production present in all incubators. Any decrease in the slope of the regression from unity is a measure of the fractional inhibition of primary production by selected UVR bandwidth. Primary production measurements under all UV treatments were well correlated to the primary production measurements under Q_{PAR} only (average r^2 = 0.97 ± 0.01). The average daily inhibition by UVR was 34.3 ± 2.6% (n = 10) and decreased with the progressive removal of the shorter wavelengths of UVR (Table 2). The value for the inhibition due to the radiation removed by T314, which can be considered to approximate UV-B radiation, was 14.6%, or 43% of the total UVR inhibition. By difference, UV-A radiation was responsible for 19.7% inhibition of photosynthetic potential, though radiation between 383 and 402 nm appeared to slightly enhance primary production (Table 2).

To estimate the goodness of the linear fit used to estimate FI_{Tnm}, we analyzed the residuals (measured minus predicted values) normalized to the predicted value (Fig. 6B). A positive residual implied that the

Table 2. September 16 (Day 259 of the Year), 1993: comparison of the primary production hourly rates, assimilation rates and doubling times of surface phytoplankton communities collected from LTER Stn B and maintained in simulated *in situ* incubators differing only in the spectral light treatment. The inhibition estimates were based on changes in primary production relative to the PAR only (P_{T402}) treatment

Outdoor incubator	Volumetric primary production (mg C m^{-3} h^{-1})	Assimilation rate (mg C mg chl^{-1} h^{-1})	Doubling time (d)[a]	Measured daily averaged inhibition relative to P_{PAR} (%)	Modeled daily averaged inhibition relative to P_{PAR} (%)[b]
T299	0.33 ± 0.02	1.82 ± 0.03	6.3 ± 0.8	34.3 ± 2.6	31.4 ± 3.0
T314	0.40 ± 0.02	2.18 ± 0.03	5.3 ± 0.7	22.4 ± 2.4	26.4 ± 2.5
T324	0.40 ± 0.02	2.18 ± 0.04	5.3 ± 0.7	19.7 ± 2.7	19.7 ± 1.9
T328	0.48 ± 0.04	2.61 ± 0.10	4.4 ± 0.6	12.9 ± 2.3	12.2 ± 1.1
T383	0.53 ± 0.02	2.89 ± 0.07	4.0 ± 0.5	-0.02 ± 0.12	-0.01 ± 0.0
T402	0.54 ± 0.09	2.94 ± 0.26	3.9 ± 0.6	0	0
Indoor photosynthetron	0.55 ± 0.13	3.03 ± 0.41	3.8 ± 0.7	-	-

[a]Carbon-based estimates over the incubation time given a measured C/chl ratio of 398 ± 50 w/w. The particulate carbon content represents the average concentration at the surface for the 3 d prior to the experiment

[b]Modelled estimates were determined using Eqs. (3) & (4)

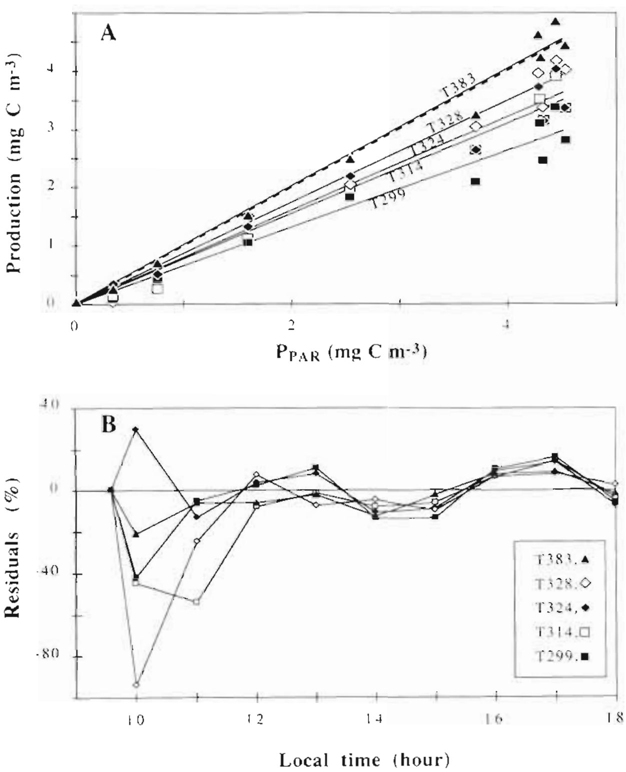

Fig. 6. (A) Regressions of cumulative primary production for each UV light treatments against cumulative primary production measured in the absence of UV radiation (T402 incubator). See text for the slope and the regression coefficient of the best-fit lines for each treatment. Note that the 1:1 line is not discernible from the T383 vs T402 regression line. (B) Percent residuals of regressions in upper figure as a function of time of the day

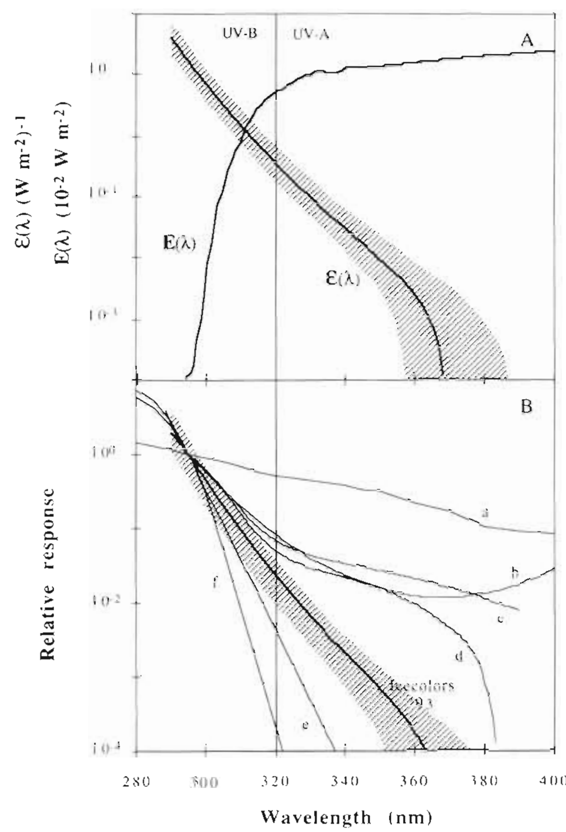

Fig. 7 (A) Comparison of the daily averaged BWF for the *in situ* inhibition of primary production by UV radiation ε(λ) and the average irradiance over the incubation time *E*(λ). (B) Comparison between the BWF for the inhibition of carbon uptake in Antarctic phytoplankton assemblages ('Icecolors 93') and action spectra describing the UV sensitivity of: (a) the Hill reaction in chloroplasts (Jones et al. 1966, redrawn from Smith & Baker 1982); (b) the oxygen evolution in a leaf of *Rumex patienta* (Caldwell 1986, redrawn from Rundel 1983), the carbon uptake in laboratory culture of a temperate latitude (Cullen et al. 1992); (c) diatom (*Phaedactylum* sp.) and (d) dinoflagellate (*Prorocentrum micans*); (e) DNA damage in anchovy eggs and larvae (Hunter 1979, redrawn from Smith & Baker 1982); and (f) the naked DNA damage as originally described by Setlow (1974)

phytoplankton were less sensitive to the different UVR exposures than what would be predicted from a linear fit. Results showed that the percent residuals decreased with time, following the increase in the cumulative signal to noise ratio. Although the absolute residuals were small for incubation greater than 2 h, they represented a significant fraction of the signal (~10%) and did display a systematic diurnal deviation.

BWF and RAF for Antarctic phytoplankton

The daily average *in situ* BWF for the present study of Antarctic phytoplankton was deconvoluted from the knowledge of the 5 broadband daily inhibition values ($FI_{T_{nnn}}$) and the corresponding average spectral irradiances responsible for the damage (Fig. 7A). The phytoplankton sensitivity to shortest wavelengths of UVR decreased approximately exponentially as wavelength increased. Best fit to the data was obtained with a double exponential decay function, negatively offset to allow for enhancement of primary production by the longest wavelengths of UVR, expressed as:

$$\varepsilon(\lambda) = \exp(a + b\lambda + c\lambda^2) + m \quad (7)$$

The parameters describing the daily integrated BWF $\varepsilon(\lambda)$ [(W m^{-2})$^{-1}$] are: a = 119.65, b = -6.223×10^{-1}, c = 7.670×10^{-4} nm^{-2}, m = -4.03×10^{-3}; and those describing the chl-specific function $\varepsilon^{*}(\lambda)$ [mg C mg chl^{-1} (J m^{-2})$^{-1}$] are: a = 112.5, b = -6.223×10^{-1}, c = 7.670×10^{-4}, m = -3.17×10^{-6} with χ^2 = 0.212 (p = 0.0052). The associated RAF (Eq. 5) for the BWF on this date was 0.91 ± 0.3 units.

Quantifying how sensitive the determination of the BWF was to a change in the inhibition input parame-

ters FI_{Tnm} required a realistic estimate of the error around FI_{Tnm} as well as a way to quantify the associated change in the BWF. We chose the RAF as an estimator of the general shape of the BWF As described above, the residuals from the linear fit used to determine FI_{Tnm} represented ~10% of the signal. To estimate the sensitivity of the BWF algorithm to the input parameters, we determined the impact of ±10% variation in each FI_{Tnm} on the RAF. These 10 manipulated BWFs had associated RAFs ranging from 0.87 to 0.96, representing an average 2.4% change from the original RAF.

DISCUSSION

The negative impact of UV radiation on phytoplankton short-term production is widely accepted (El-Sayed et al. 1990, Karentz 1991, Karentz et al. 1991a, Helbling et al. 1992, Smith et al. 1992, Bothwell et al. 1993, Holm-Hansen et al. 1993, Bothwell et al. 1994, Prézelin et al. 1994b) and the degree of inhibition appears relatively consistent between workers (Prézelin et al. 1994a). The present study quantifies the degree to which several UV broadbands decrease short-term estimates of primary production under simulated *in situ* conditions and provides an estimate of the spectral variation of the inhibition of Antarctic phytoplankton under conditions of enhanced levels of UV-B radiation. We discuss the shape of newly deconvoluted biological weighting in comparison with action spectra for other processes, explain how such a function can be used to estimate the UV effect of the Antarctic ozone hole on primary production and test its application to correct PAR-dependent measurements of Antarctic primary production with the sole knowledge of the spectral UV field.

A comparison of the principal published BWFs normalized to 295 nm is presented in Fig. 7B. The slope of the functions at the lowest wavelengths depicts the sensitivity of each process studied to the unbalanced increase in UVR associated with the depletion of ozone. The RAF quantifies this sensitivity by directly relating the increase in damage due to the decrease in ozone. At the end of the austral winter, Antarctic phytoplankton appeared more susceptible to an increase in the Q_{UVB}/Q_{UVA} balance than temperate terrestrial plants (Jones & Kok 1966, Caldwell 1971) and temperate marine phytoplankton (Cullen et al. 1992). The RAF for Antarctic phytoplankton production (0.91 ± 0.3 units) lies in the upper region of the range in RAFs measured for various plant damages (as tabulated by Madronich 1993). It was 40% higher than the RAFs measured for the inhibition of photosynthesis in 2 temperate phytoplankton species in culture (Cullen et al. 1992). Whether this enhanced sensitivity is a result of a change in species composition, the exposure history or the experiment conditions remains to be established and is under ongoing investigation.

On the contrary, the RAFs associated with the 2 DNA action spectra (Setlow 1974, Hunter 1979) as well as all RAFs determined for other DNA-related effects (Madronich 1993) were much greater than our estimate. BWF are a function of the absorption spectra of the target molecule and the negative impact of the energy absorbed onto the process studied (e.g. quantum yield of inhibition). As a consequence, BWFs describing the UV damage of different target molecules are not constant, since the absorption spectra of the molecules are different. With whole organisms, the issue is further complicated by photoprotective absorption and photoprocesses countering the inhibition effects. For instance, in the case of plant carbon production, the sensitivity of the cells will decrease with intracellular photoprotectant concentration or with changes in the rates of counterprocesses such as photosynthesis (Tevini & Teramura 1989, Prézelin et al. 1993) or photorepair (Karentz et al. 1991a, b, Raven 1991). It is therefore not surprising to find intact plant photosynthetic machinery to be less sensitive to UV radiation than naked DNA.

With the knowledge of the BWF, the *in situ* spectral irradiance and the primary production under PAR (P_{PAR}), one can estimate UV-dependent rates of primary production (Eqs. 3 & 4). The description of the earth surface UV climatology has greatly improved in recent years due to the development of radiative transfer models and monitoring networks (Smith & Wan 1992, Madronich 1993, Booth et al. 1994). Primary production of the oceans remains difficult to characterize due to its large temporal and spatial variability. In recent years, parameterizations of the variation of carbon uptake with increasing irradiance (*P-I* curves) have become a common way to describe ocean productivity in the field. This technique has been preferred over *in situ* incubations because it allows for high frequency sampling strategies and is very suited to studying the effects of environmental factors on phytoplankton production (Cote & Platt 1983, 1984, Prézelin et al. 1987, Smith et al. 1987, Platt & Gallegos 1988, Prézelin et al. 1992). There is evidence that short incubations often overestimate daily *in situ* primary production. A commonly evoked mechanism is that *P-I* curves are a measure of gross production, whereas some fixed radiolabelled carbon can be catalyzed through respiration during long-term incubations, progressively lowering determination to net production values. Another inherent problem of laboratory incubations is the spectral bias introduced by the use of an artificial light source (Kiefer & Strickland 1970, Loh-

renz et al. 1992). One of the effects commonly investigated is the red-light enrichment associated with use of a tungsten light source replacing the 'bluer' *in situ* light field. Another bias is the removal of the damaging ultraviolet radiation by the laboratory incubators, the samples being incubated under PAR only. Results from our experiment show that, after a 2 h incubation under PAR, no significant difference in *P-I* parameters were detected between samples originating from different UV treatments. Furthermore, the time course of primary production as modeled using the diurnal variation of the *P-I* parameters (P_i, Eq. 1) closely approximated primary production measured in the PAR-only incubator (T402, Fig. 8). This demonstrates that most of the production enhancement in the short-term incubations was due to the removal of UV light and that a 2 h incubation under PAR only was sufficient to release the cells from the UV stress to a degree which made any decrease in photosynthetic potential not detectable with the precision of our method. This is consistent with the theory that the 32 kDa photosystem II reaction center protein, which is rapidly turned over (half-life < 25 min) in the presence of visible light (Rogers et al. 1986, Greenberg et al. 1989), is the main photosynthetic machinery target degraded under UV radiation in higher plants (Greenberg et al. 1989) and in phytoplankton (Schofield et al. 1995). Therefore, *P-I* measurements over long incubations (2 h) provide a way to model *in situ* primary production under PAR light only (P_{PAR}). One caveat is that only *P-I* curves determined over short incubation (<30 min) will reflect UV stress if incubated without UV. Another is that natural phytoplankton populations are likely to recover from some of the reversible damages at dawn and dusk, when the UVR/PAR ratio is low. The degree to which the cost of the repair decreases long-term growth remains to be investigated.

With estimates of irradiance field, PAR-dependent rates of photosynthesis and the BWF, we can now model UV-dependent rates of photosynthesis using Eqs. (3) & (4). To examine the model's applicability in reproducing diurnal patterns of UV-dependent primary production and its adaptability to changes in the UV-B to UV-A balance in the external light field, 2 tests were applied. In a first internal test, we compared the modeled UV-dependent rates of primary production with the measured values in the 6 incubators (Fig. 8). Modeled primary production was calculated using the daily average BWF and PAR-dependent rates of photosynthesis determined either from the primary production of samples exposed to PAR only (PT402) or primary production modeled from *P-I* estimates (P_i). Good agreement (within 3% on average) was found between the 2 models and the diurnal patterns were similar. Differences in incubation lengths between the 2 h *P-I* and the cumulative daily incubations could introduce differences on the sole basis of gross versus net photosynthesis. The similarity of the diurnal pattern of both measurements (Fig. 8) suggests, however, that such differences were not observed. Within the experiment

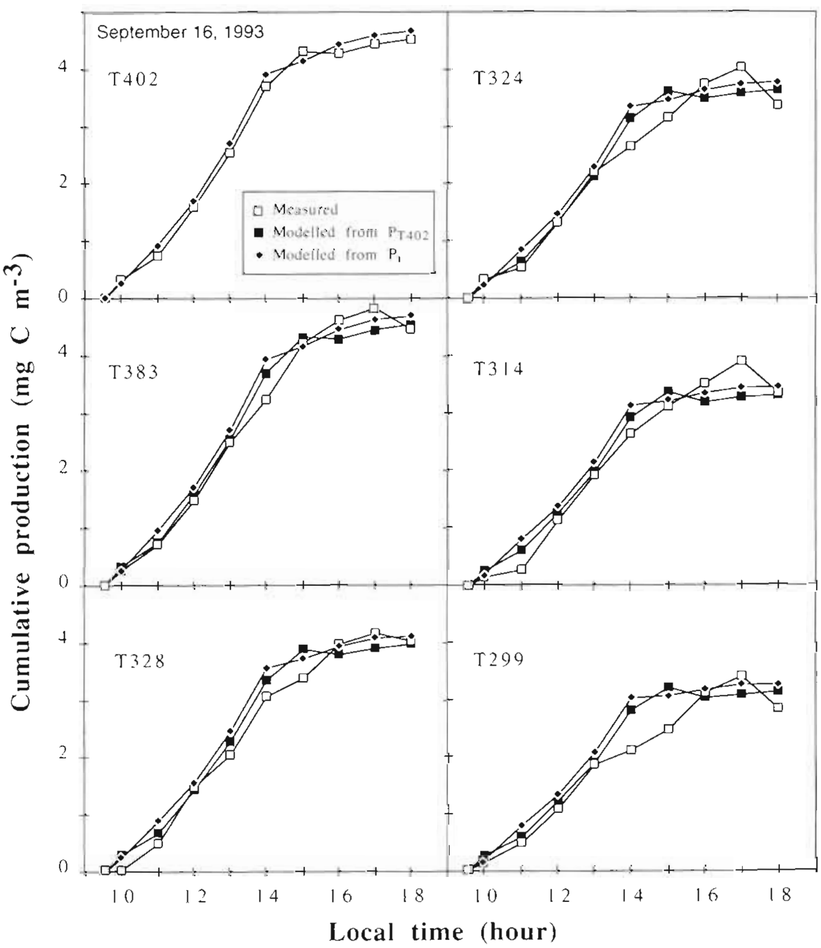

Fig. 8. Comparison between the time course of measured and modeled *in situ* primary production in the different UV treatments of Antarctic phytoplankton collected on September 16, 1993. Primary production was modelled from the knowledge of the BWF, the UV spectral irradiance over the incubation time and the primary production under PAR radiation only, P_{PAR} (Eqs. 2 & 5). P_{PAR} was either measured in the T402 incubator (P_{T402}) or modelled from the *P-I* parameters using Eq. (1) (P_i). See text for details

conditions, *P-I* values were, therefore, good estimators of primary production released from UV stress.

Time courses of modeled primary production in all UV treatments compared well with the measured values although some deviations were apparent, especially for the lowest wavelength of UVR (T299). Such deviations, also observed in the residuals plot (Fig. 6), are a reflection of the diurnal variation of the quantum requirement for inhibition, particularly enhanced in our experiment by the extreme fluctuation in weather pattern (Fig. 3). Even though UV inhibition of production does vary diurnally, using a constant BWF over the course of 1 d will, in a first approximation, provide accurate estimates of *in situ* inhibition of primary production, as shown from the correlation (r^2 = 0.97, n = 54) between modeled and measured estimates.

In a second external test, we used the BWF to compare modeled estimates of *in situ* primary production to hourly measurements made in 2 incubators (T299 and T328) on a different day (September 9, 1994). On that day, the phytoplankton assemblages and the ice coverage were similar to September 16. Stratospheric ozone concentration, however, was reduced to 205 DU, resulting in an increase in the UV-B to UV-A ratio and thus providing a good test of the spectral robustness of the model. The total measured inhibition was 26.7%, 15.8% of which was due to UV-A radiation. The model very closely estimated daily results from ^{14}C measurements, with a modeled total inhibition of 26.6% and a slightly enhanced UV-B to total inhibition ratio (50.4 vs 40.8%). Similarly, the diurnal variation of modeled UV-dependent rates of primary production (Fig 9) compared well with the measured values (r^2 = 0.97, n = 10 for T299; r^2 = 0.99, n = 10 for T328).

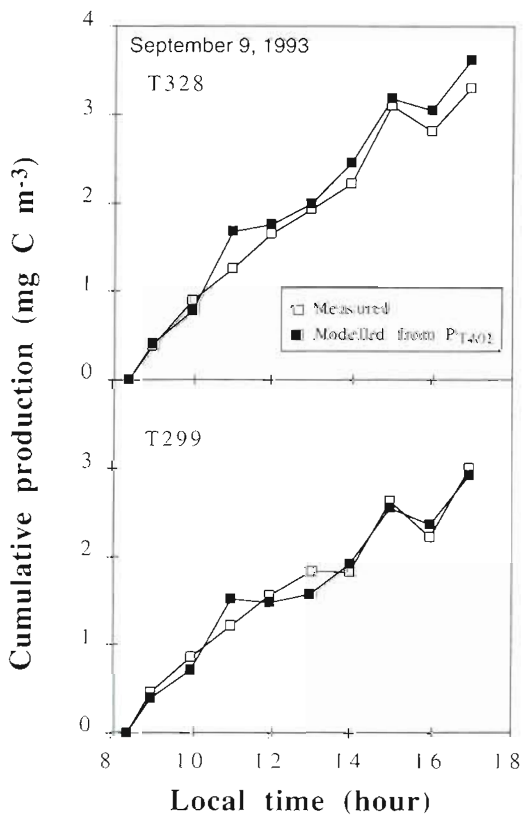

Fig. 9. Comparison between the time course of measured and modelled primary production in the 2 UV treatments (T299, T328) on September 9, 1993. Primary production was modelled from the knowledge of the BWF, the UV spectral irradiance over the incubation time and the primary production under PAR only, $P_{...}$ (Eqs. 2 & 5)

Predictions of UV-dependent rates of primary production in natural Antarctic phytoplankton communities are possible, given that *in situ* production in the absence of UV radiation and UV fluence rates on a time and space scale matching production estimates are available. The *in situ* BWF provides a valuable tool to emulate primary production under fluctuating levels of the UV-B to UV-A ratio. Further information, however, must be gathered about the behavior of the BWF and its predictive limits, particularly with varying community structure and light history.

Acknowledgements. Research support was provided by the National Science Foundation grant DPP-92-20962 awarded to B.B.P. We thank A. Matlick for his technical support, T. J. Evans, B. Kroon, R. Jovine, M. Moline, O. Schofield and the women and men of Palmer Station for assistance with the field work. R. Booth for making the irradiance data readily available to us and Drs S. Madronich and R. C. Smith for providing helpful discussions, reviews and encouragement.

LITERATURE CITED

Booth CR, Lucas TB, Morrow JH, Weiler SC, Penhale PA (1994) The United States National Science Foundation's polar network for monitoring ultraviolet radiation. In: Weiler S, Penhale P (eds) Ultraviolet radiation and biological research in Antarctica. Antarctic Research Series, Vol 62. American Geophysical Union, Washington, DC, p 17–37

Booth CR, Madronich S (1994) Radiation amplification factors --improved formulation accounts for large increases in ultraviolet radiation associated with Antarctic ozone depletion. In: Weiler S, Penhale P (eds) Ultraviolet radiation and biological research in Antarctica. Antarctic Research Series, Vol 62. American Geophysical Union, Washington, DC, p 39–42

Bothwell, ML, Sherbot DMJ, Pollock CM (1994) Ecosystem response to solar ultraviolet-B radiation: influence of trophic-level interactions. Science 265:97–100

Bothwell ML, Sherbot DMJ, Roberge AC, Daley RJ (1993) Influence of natural radiation on lotic periphytic diatom community growth, biomass accrual, and species composition: short-term versus long-term effects. J Phycol 29: 24–35

Caldwell MM (1971) Solar ultraviolet radiation and the growth and development of higher plant. In: Giese A (ed) Photophysiology, Vol 6. Academic Press, New York, p 131–177

Caldwell MM, Camp LB, Warner CW, Flint SD (1986) Action spectra and their key role in assessing biological consequences of solar UV-B radiation change. In: Worrest RC, Caldwell MM (eds) Stratospheric ozone reduction, solar ultraviolet radiation and plant life. NATO ASI series G8, Springler-Verlag, Berlin, p 87–111

Cote B, Platt T (1983) Day-to-day variations in the spring-summer photosynthetic parameters of coastal marine phytoplankton. Limnol Oceanogr 28:320–344

Cote B, Platt T (1984) Utility of the light-saturation curve as an operational model for quantifying the effects of environmental conditions on phytoplankton photosynthesis. PSZN I: Mar Ecol 18:57–66

Cullen JJ, Neale PJ, Lesser MP (1992) Biological weighting function for the inhibition of phytoplankton photosynthesis by ultraviolet radiation. Science 258:646–650

El-Sayed SZ, Stephens FC, Bidigare RR, Ondrusek ME (1990) Effects of ultraviolet radiation on Antarctic marine phytoplankton. In: Kerry KR, Hempel G (eds) Antarctic ecosystems: ecological change and conservation. Springer-Verlag, New York, p 379–385

Greenberg BM, Gaba V, Canaani O, Malkan S, Mattoo AK (1989) Separate photosynthetiser mediate degradation of the 32-kDa photosystem II reaction center protein in the visible and UV spectral regions. Proc Nat Acad Sci USA 86:6617–6620

Helbling WE, Villafañe V, Ferrario M, Holm-Hansen O (1992) Impact of natural ultraviolet radiation on rates of photsynthesis and on specific marine phytoplankton species. Mar Ecol Prog Ser 80:89–100

Holm-Hansen O, Helbling EW, Lubin D (1993) Ultraviolet radiation in Antarctica—inhibition of primary production. Photochem Photobiol 58:567–570

Hunter JH, Taylor JH, Moser HG (1979) The effect of ultraviolet irradiation on eggs and larvae of the northern anchovy, *Engraulis mordax*, and the pacific mackerel, *Scomber japonicus*, during the embryonic stage. Photochem Photobiol 29:325–338

Jones LW, Kok B (1966) Photoinhibition of chloroplast reactions. II. Multiple effects. Plant Physiol 41:1044–1049

Karentz D (1991) Ecological considerations of Antarctic ozone depletion. Antarctic Science 3:3–11

Karentz D, Cleaver JE, Mitchell DL (1991a) Cell survival characteristics and molecular responses of Antarctic phytoplankton to ultraviolet-B radiation. J Phycol 27:326–341

Karentz D, Cleaver JE, Mitchell DL (1991b) DNA damage in the Antarctic. Nature 350:28

Kiefer D, Strickland JDH (1970) A comparative study of photosynthesis in sea water samples incubated under two types of light attenuator Limnol Oceanogr 15:408–412

Krebbs WN (1983) Ecology of neretic marine diatoms in Arthur Harbor, Antarctica. Micropaleontology 29:267–297

Lewis, MR, Cullen JJ, Platt, T (1984) Relationship between vertical mixing and photoadaptation of phytoplankton: similarity criteria. Mar Ecol Prog Ser 15:141–149

Lohrenz SE, Weisenburg DA, Rein CR, Arnone RA, Taylor CD, Knauer GA, Knap QH (1992) A comparison of *in situ* and simulated *in situ* methods for estimating oceanic primary production. J Plankton Res 14:201–221

Lubin D, Frederick JE (1991) The ultraviolet radiation environment of the Antarctic Peninsula: the roles of ozone and cloud cover. J Appl Meteorol 30:478–493

Madronich S (1993) UV radiation in the natural and the perturbed atmosphere. In: Tevini M (ed) UV-B radiation and ozone depletion. Lewis, Boca Raton, FL, p 17–69

Madronich S, de Gruijl FR (1993) Skin cancer and UV radiation. Nature 366:23

Middleton EM, Teramura AH (1994) Understanding photosynthesis, pigment and growth responses induced by UV-B and UV-A irradiances. Photochem Photobiol 60: 38–45

Mohr H, Drumm-Herrel H, Öelmüller R (1984) Coaction of phytochrome and blue/UV light photoreceptors. In: Spenger H (ed) Blue light responses: phenomena and occurrence in plants and microorganisms, Vol 1 CRC Press, Boca Raton, FL, p 6–19

Moline MA, Prézelin BB, Schofield O, Smith RC (1997) Temporal dynamics of coastal Antarctic phytoplankton: environmental driving forces and impact of a 1991–1992 summer diatom bloom on the nutrient and light regimes. In: Battaglia B, Valencia J, Walton DWH (eds) Antarctic communities. Cambridge University Press (in press)

National Academy of Sciences (1979) Protection against depletion of stratospheric ozone by chlorofluorocarbons. National Academy Press, Washington, DC

Neale PJ, Richerson PJ (1987) Photoinhibition and the diurnal variation of phytoplankton photosynthesis. I. Development of a photosynthesis-irradiance model from studies of *in situ* responses. J Plankton Res 9:167–193

Parsons T, Maita Y, Lalli C (1984) A manual of chemical and biological methods for sea water analysis. Pergamon Press, Oxford

Platt T, Gallegos CL (1988) Modelling primary production. In: PG Falkowski (ed) Primary productivity in the sea. Plenum Press, New York, p 339–362

Prézelin BB, Bidigare RR, Matlick HA, Putt M, Ver Hoven B (1987) Diurnal patterns of size fractioned primary productivity across a coastal front. Mar Biol 4:563–574

Prézelin BB, Boucher NP, Moline MA, Stephens E, Seydel K, Scheppe K (1992) Palmer LTER program: spatial variability in phytoplankton and surface photosynthetic potential within the Peninsula grid, November 1991 Antarct J US 27:242–245

Prézelin BB, Boucher NP, Schofield O (1994a) Evaluation of field studies of UV-B radiation effects on Antarctic marine primary productivity. In: Bigg H, Joyner MEB (eds) Stratospheric ozone depletion/UV-B radiation in the biosphere, Vol 118. NATO Advance Study Institute Series, p 181–194

Prézelin BB, Boucher NP, Smith RC (1993) Daytime kinetics of UVA and UVB inhibition of photosynthetic activity in Antarctic surface waters. In: Yamamoto HY, Smith CM (eds) Special symposium on photosynthetic responses to the environment. Current Topics in Plant Physiology. Plant Physiology Series, Vol 8, p 150–155

Prézelin BB, Boucher NP, Smith RC (1994b) Marine primary production under the influence of the Antarctic ozone hole: Icecolors '90. In: Weiler S, Penhale P (eds) Ultraviolet radiation and biological research in Antarctica, Vol 62. American Geophysical Union, Washington, DC, p 159–186

Prézelin BB, Glover HE, Ver Hoven BM, Steinberg D, Matlick HA, Schofield O, Nelson NB, Wyman M, Campbell L (1989) Blue-green light effects of light-limited rates of photosynthesis: relationship to pigmentation and productivity estimates for *Synechococcus* populations from the Sargasso Sea. Mar Ecol Prog Ser 54:121–136

Raven JA (1991) Responses of aquatic photosynthetic organisms to increased solar UVB. J Photochem Photobiol, B: Biol 9:239–244

Rogers S, Well R, Rechsteiner M (1986) Amino acid sequences common to rapidly degraded proteins: the PEST hypothesis. Science 234:364–368

Roy CR, Gies HP, Tomlinson DW, Lugg DL (1994) Effects of ozone depletion on the ultraviolet radiation environment at the Australian stations in Antarctica. In: Weiler S, Pen-

hale P (eds) Ultraviolet radiation and biological research in Antarctica, Vol 62. American Geophysical Union, Washington, DC, p 1–15
Rundel RD (1983) Action spectra and estimation of biologically effective UV radiation. Physiol Plant 58:360–366
Schofield O, Prézelin BB, Kroon BA (1995) Impact of ultraviolet-B radiation on photosystem II and its relationship to the inhibition of carbon fixation rates for Antarctic ice algae communities. J Phycol 31:703–715
Schofield O, Prézelin BB, Smith RC, Stegmann PM, Nelson NB, Lewis MR, Baker KS (1991) Variability in spectral and nonspectral measurements of photosynthetic light utilization efficiencies. Mar Ecol Prog Ser 78:253–271
Senger H, Schmidt W (1986) Diversity of photoreceptors. In: Kendrick RE, Kronenberg GHM (eds) Photomorphogenesis of plants. Martinus Nijhoff/Dr W Junk Publishers, Dordrecht, p 137–158
Setlow RB (1974) The wavelength in sunlight effective in producing skin cancer: a theoretical analysis. Proc Nat Acad Sci USA 71:3363–3366
Smith RC, Baker KS (1982) Assessment of the influence of enhanced UV-B on marine primary productivity. In: Calkins J (ed) The role of solar ultraviolet in marine ecosystems. Plenum, New York, p 509–537
Smith RC, Bidigare RR, Prézelin BB, Baker KS, Brooks JM (1987) Optical characterization of primary productivity across a coastal front. Mar Biol 96:575–591
Smith RC, Prézelin BB, Baker KS, Bidigare RR, Boucher NP, Coley T, Karentz D, MacIntyre S, Matlick HA, Menzies D, Ondrusek M, Wan Z, Waters KJ (1992) Ozone depletion: ultraviolet radiation and phytoplankton biology in Antarctic waters. Science 258:952–959
Smith RC, Wan Z (1992) Ozone depletion in Antarctica: modeling its effect on solar UV irradiance under clear-sky conditions. J Geophys Res 97:7383–7397
Stolarski RS, Bojkov R, Bishop L, Zerefos C, Staehelin J, Zawondny J (1992) Measured trends in stratospheric ozone. Science 256:342–349
Tevini M, Teramura AH (1989) UV-B effects on terrestrial plants. Photochem Photobiol 50:479–487
UNEP (1994) Environmental effects of stratospheric ozone depletion—1994 assessment. Van der Leun JC, Teramura AH, Tevini M (eds) United Nation Environment Programme, Nairobi
Weiler S, Penhale P (1994) Ultraviolet radiation and biological research in Antarctica. Antarctic Research Series, Vol 62. American Geophysical Union, Washington, DC
WMO (World Meteorological Organization) (1995) Scientific assessment of ozone depletion. Global Ozone Research and Monitoring Project, Rept 37. Geneva
Zimmermann RC, Beeler SooHoo J, Kremer JN, D'Argenio DZ (1987) Evaluation of variance approximation techniques for non-linear photosynthesis-irradiance models. Mar Biol 95:209–215

This article was submitted to the editor

Manuscript first received: December 28, 1995
Revised version accepted: September 16, 1996